Received: 17 March 2018 | Revised: 12 December 2018 | Accepted: 26 February 2019

DOI: 10.1002/joc.6057

International Journal of Climatology RMetS

RESEARCH ARTICLE

Modulation of wet-season rainfall over Iran by the Madden–Julian Oscillation, Indian Ocean Dipole and El Niño–Southern Oscillation

Farnaz Pourasghar[1] | **Eric C. J. Oliver**[2,3,4] | **Neil J. Holbrook**[3,4]

[1]Research Department, Bureau of Meteorology, Tabriz, Iran

[2]Department of Oceanography, Dalhousie University, Halifax, Nova Scotia, Canada

[3]Institute for Marine and Antarctic Studies, University of Tasmania, Hobart, Tasmania, Australia

[4]ARC Centre of Excellence for Climate Extremes, University of Tasmania, Hobart, Tasmania, Australia

Correspondence
Farnaz Pourasghar, Bureau of Meteorology, Tabriz, Iran.
Email: farnaz_pourasghar@yahoo.com

The intra-seasonal variation of precipitation over Iran is examined in terms of the combined effects of the Madden–Julian Oscillation (MJO), Indian Ocean Dipole (IOD) and El Niño–Southern Oscillation (ENSO), using daily observations during the wet season (October–May) from 1961 to 2015. We have examined how the probability of daily rainfall above the upper tercile varies across MJO phases during positive and negative IOD and ENSO states. The results indicate that the response of Iran's wet-season rainfall to the MJO is affected more by large-scale atmospheric variations associated with the IOD than by ENSO. The negative (positive) IOD strengthens (suppresses) the MJO–rainfall relationship in the wet and dry MJO phases. The variation in the atmospheric variables (relative humidity and vertical velocity) indicates more (less) humidity and upwards (downwards) motion which increases (decreases) precipitation in wet (dry) MJO phases during the negative IOD. The rainfall relationship with the MJO during the negative IOD is statistically significant, while the relationship during the positive IOD is weak; and no significant relationship is found during either phase of ENSO.

KEYWORDS

Indian Ocean Dipole, intra-seasonal variability, Madden–Julian Oscillation, rainfall probability

1 | INTRODUCTION

The Middle East and southwestern Asia are regions that are water stressed and prone to severe droughts. This leads to social and economic vulnerabilities to water scarcity (Barlow *et al.*, 2016). Iran's climate is characterized by low precipitation (annual rainfall is about 240 mm) with variability on daily, seasonal and inter-annual timescales—including extremes and prolonged droughts and floods (Raziei *et al.*, 2009; Madani, 2014; Khalili *et al.*, 2016). Owing to the complex orography and wide latitudinal extent, from the Hadley cell descending branch north to mid-latitudes, precipitation in Iran is highly variable both in space and time (Raziei *et al.*, 2012). The maximum annual rainfall of about 1,800 mm occurs on the Caspian seashore, while about 400 mm of annual rainfall occurs in the sloping region of the Alborz and Zagros mountains. Annual rainfall averages decrease to <100 mm depending on the location in the central and eastern part of Iran (Soltani *et al.*, 2012). About 90% of the annual precipitation over Iran occurs from October to May (except the Caspian seashore where it is 75%). Hence, improving our understanding of relevant climatic relationships and predictors of inter-annual and intra-seasonal precipitation variations is essential in order to aid water security and agricultural decision-making in Iran.

Raziei *et al.* (2012) investigated the influence of large-scale atmospheric circulation on seasonal regimes of daily precipitation over Iran. Their results suggest that the spatial distribution of precipitation over Iran is largely governed by the geographical location of both the mid-tropospheric trough over the Middle East and the Arabian anticyclone. Rousta *et al*. (2016) analysed extreme rainfall events in the central plateau of Iran. The synoptic findings indicate that two patterns of deep troughs and high ridges in the eastern Mediterranean Sea region were responsible for driving the heavy precipitation events over the central plateau of Iran. Their results suggest that the main moisture resources for the rainy systems in the first pattern (deep trough) including the Persian Gulf, Oman Sea, Indian Ocean and Red Sea, while for the second pattern (high ridge), the Persian Gulf and Red Sea play a significant role in feeding the storms in the central regions of Iran. Moreover, the southwards movement of the Polar Vortex is also considered as an important factor in producing extreme precipitation events over the central plateau of Iran.

Previous studies have shown the linkage between large-scale teleconnection indices and climate variables over Iran. The El Niño–Southern Oscillation (ENSO) has been suggested to be the important inter-annual climate mode that affects rainfall variability over the region (Nazemosadat and Cordery, 2000; Nazemosadat *et al*., 2006; Raziei *et al*., 2009). Nazemosadat and Ghasemi (2004) showed that compared to the neutral period, drought intensity is generally much smaller, and most parts of Iran tend to experience wet conditions when warm ENSO prevails (the seasonal Southern Oscillation Index is the upper 25% of all observed values). On the other hand, when a vigorous La Niña prevails, the chance of wet conditions is low and dry conditions high. The probability of severe autumnal drought is increased in strong La Niña events. During winters of warm ENSO phases (El Niño), although most of the country receives precipitation above the drought threshold, in the southeastern and northwestern districts of Iran, the risk of winter drought is high. Roghani *et al*. (2016) also investigated the relationship between ENSO and autumn rainfall in Iran. Their results showed that El Niño and La Niña phases are associated with increased and decreased autumn rainfall, respectively, in the north, northwest and western regions of Iran. In contrast, Pourasghar *et al*. (2012) showed that inter-annual variations of precipitation in autumn and early winter are significantly correlated with the Indian Ocean Dipole (IOD), but not with ENSO, and during the latter part of the wet season it is influenced by modes of variability over the Mediterranean Sea.

The Arabian anticyclone plays an important role in controlling the spatial pattern of precipitation over Iran. The southeasterly moisture flux anomaly over the Arabian Sea turns anticyclonically and transport more moisture to the southern part of Iran from the Arabian Sea, the Red Sea and the Persian Gulf during the positive IOD. On the other hand, the moisture flux has a northerly anomaly over Iran during the negative IOD, which results in reduced moisture supply from the south. On intra-seasonal timescales, the Madden–Julian Oscillation (MJO) is the leading mode of tropical intra-seasonal variability in the atmosphere. Pourasghar *et al*. (2015) analysed daily precipitation data in the southern part of Iran and showed wet conditions tend to prevail during MJO phases 1, 2, 7 and 8. The geographical position of the mid-tropospheric trough and high pressure over the Arabian Sea and South Asia are major contributors to the anomalous moisture transport. The northwards and onshore moisture flux anomalies transport more moisture from the Arabian Sea, the Gulf of Aden and the Red Sea to southern Iran. The western-high and eastern-low patterns are found for 500-hPa geopotential height anomalies in MJO phases 3–6, indicating northerly and offshore moisture flux anomalies. These patterns reduce moisture supply to southern Iran. Vertical velocity anomalies also vary with the eastwards propagation of the MJO. Nazemosadat and Shahgholian (2017) analysed characteristics of heavy precipitation in south western Iran and its linkage to the MJO. The highest frequency of heavy precipitation is related to MJO phase 8. For phases 1, 2, 7 and 8, the frequency of heavy precipitation increases significantly when the MJO amplitude is greater than unity. Formation of a strong north–south oriented cold front mainly in Saudi Arabia and west–east oriented warm fronts in the southwest of Iran were realized as the key elements for initiating heavy precipitation over the study area. Although development of the Mediterranean-based cyclonic circulation is essential for the formation of these fronts, moisture transport mostly originates from northern parts of the Arabian Sea, southern parts of the Red Sea and the Persian Gulf.

Many studies have also demonstrated that the MJO influences precipitation variability and atmospheric circulation both in the Tropics and extratropical regions, through atmospheric Rossby wave propagation (Zhang, 2005; Wheeler *et al*., 2009; Pai *et al*., 2011; Alaka and Maloney, 2012; Julia *et al*., 2012). In addition, the MJO is modulated on inter-annual timescales by ENSO (e.g., Pohl and Matthews, 2007) and potentially by the IOD (e.g., Shinoda and Han, 2005). While westerly wind bursts associated with MJO events can trigger the development of El Niño (Hendon *et al*., 2007; Seiki and Takayabu, 2007), the MJO can also be modulated by El Niño (Lin and Li, 2008; Kapur and Zhang, 2012). Additionally, it has been shown that the lifetime of the MJO is increased in La Niña years (Pohl and Matthews, 2007). Some studies have shown the influence of the IOD on the eastwards propagation of the MJO in the tropical atmosphere (Wilson *et al*., 2013; Yuan *et al*., 2014). During positive IOD years, associated with warm Sea Surface Temperature (SST) anomalies in the west and cold anomalies in the east of the tropical Indian Ocean, sub-monthly (6–30 days) wind activity near the equator and convective activity in the southeast Indian Ocean are largely reduced. During negative IOD years, sub-monthly convection is active in the southeast Indian Ocean where the anomalous convergence of surface moisture associated with these dipole events is at its maximum. The sub-monthly convection in this region is often associated with cyclonic circulation, and these disturbances propagate westwards (Shinoda and Han, 2005).

While these previous studies provide valuable information regarding the roles of individual climate modes on

Iran's precipitation, the combined effects of the IOD, ENSO and MJO in modulating Iran's rainfall are not well understood. The aim of this paper is to examine the joint modulation of intra-seasonal rainfall variations over Iran by the MJO, IOD and ENSO.

2 | DATA

2.1 | Precipitation data

Long records of daily precipitation data from January 1961 to December 2015 (54 years) for 34 stations were obtained from the Iran Meteorological Organization. The stations are well-distributed throughout the country of Iran (study area) and cover all climate zones, with high and low density in the western and southern regions (Figure 1). These long-record stations were chosen as they provided sufficient temporal coverage for the inclusion of many cycles of ENSO and the IOD. For all stations, we investigated the same period from January 1961 to December 2015.

2.2 | IOD, ENSO and MJO indices

The MJO was characterized using the historical reconstruction of the Wheeler and Hendon (2004) Real-time Multivariate MJO (RMM) index by Oliver and Thompson (2012) and Oliver (2016). The Historical Reconstruction index (IHR) is a daily reconstruction of the RMM index from 1905 to 2014 based on a multiple linear regression of 20th century reanalysis (Compo *et al*., 2011) surface pressure time series onto the RMM index, which starts in 1974. We used the IHR for 1961–2014 and the Wheeler-Hendon (RMM) index for the year 2015. These indices describe MJO activity over the Tropics, including the eastwards propagation of the corresponding large-scale anomalies. A strong MJO state is defined when the IHR amplitude is 1 or greater.

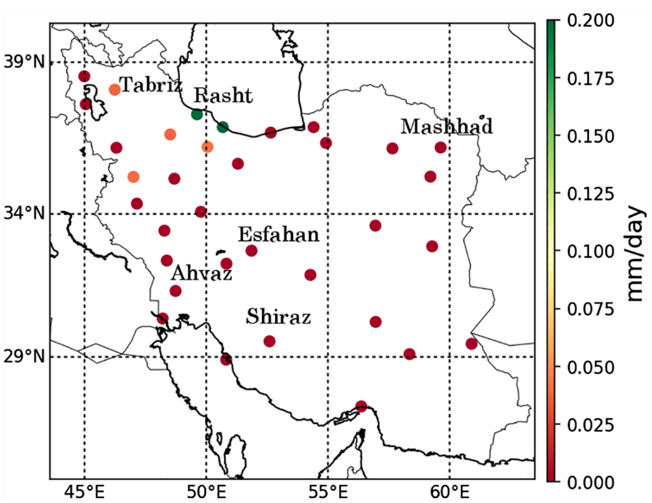

FIGURE 1 Upper tercile of daily rainfall over Iran during the wet season [Colour figure can be viewed at wileyonlinelibrary.com]

The IOD is a coupled ocean–atmosphere phenomenon in the Indian Ocean. The Dipole Mode index (DMI) is defined as the peak time (September–November) SST anomaly (SSTA) differences between the tropical western Indian Ocean (10°S–10°N, 50°–70°E) and south eastern Indian Ocean (10°S–0°, 90°–110°E) (Saji *et al*., 1999).

The Niño3 (90°–150°W, 5°S–5°N) SSTA index (otherwise known as NINO3) is a widely used indicator of eastern tropical Pacific El Niño conditions. We chose the Niño3 index as a pragmatic metric for ENSO characterization in the present study, defined for the peak period from December–February.

We assigned the monthly DMI and NINO3 index values to all days in each month. Positive (negative) IOD and El Niño (La Niña) years are defined for DMI and NINO3 index values above (below) 0.8 standard deviations, where the standard deviation was calculated over the period from 1961 to 2015 (Table 1).

2.3 | Atmospheric variables

Daily relative humidity (RH) at 600 hPa and vertical velocity at 300 hPa at 2.5 × 2.5° spatial resolution (144 × 73 grid cells globally) and precipitation rate (PR) on a T62 Gaussian grid (192 × 94) from NCEP/NCAR Reanalysis (Kalnay *et al*., 1996) were obtained for the period from 1961 to 2015. These data were used to better understand the relevant physical mechanisms underpinning precipitation variations over Iran. The study area covers 27°–38°N, 45°–61°E.

3 | METHODS

First, we examined the wet and dry seasons separately. Because we found no significant MJO–rainfall response to IOD or ENSO in the dry season, we restricted our further analysis presented here to the wet season only, that is, from October to May. The upper tercile (i.e., upper 33%) of daily rainfall during the wet season is used as the minimum critical level (threshold) for identifying wet conditions, with the threshold value (mm/day) of the tercile varying from station to station. The upper tercile at some stations is in fact 0 mm/day (Figure 1), and so we defined the baseline probability of exceeding the upper tercile as the actual probability of exceeding this value, which will be <33% at some stations (Figure 2).

TABLE 1 IOD and ENSO events based on DMI and NINO3 index value above (below) 0.8 standard deviation of peak time

Index	Positive	Negative
DMI	1961, 1963, 1967, 1972, 1982, 1987, 1991, 1994, 1997, 2002, 2006, 2007, 2008, 2011, 2012, 2014	1964, 1974, 1975, 1996
NINO3	1965/1966, 1972/1973, 1976/1977, 1982/1983, 1991/1992, 1994/1995, 1997/1998, 2009/2010	1970/1971, 1973/1974, 1975/1976, 1984/1985, 1988/1989, 1998/1999, 1999/2000, 2005/2006, 2007/2008, 2010/2011

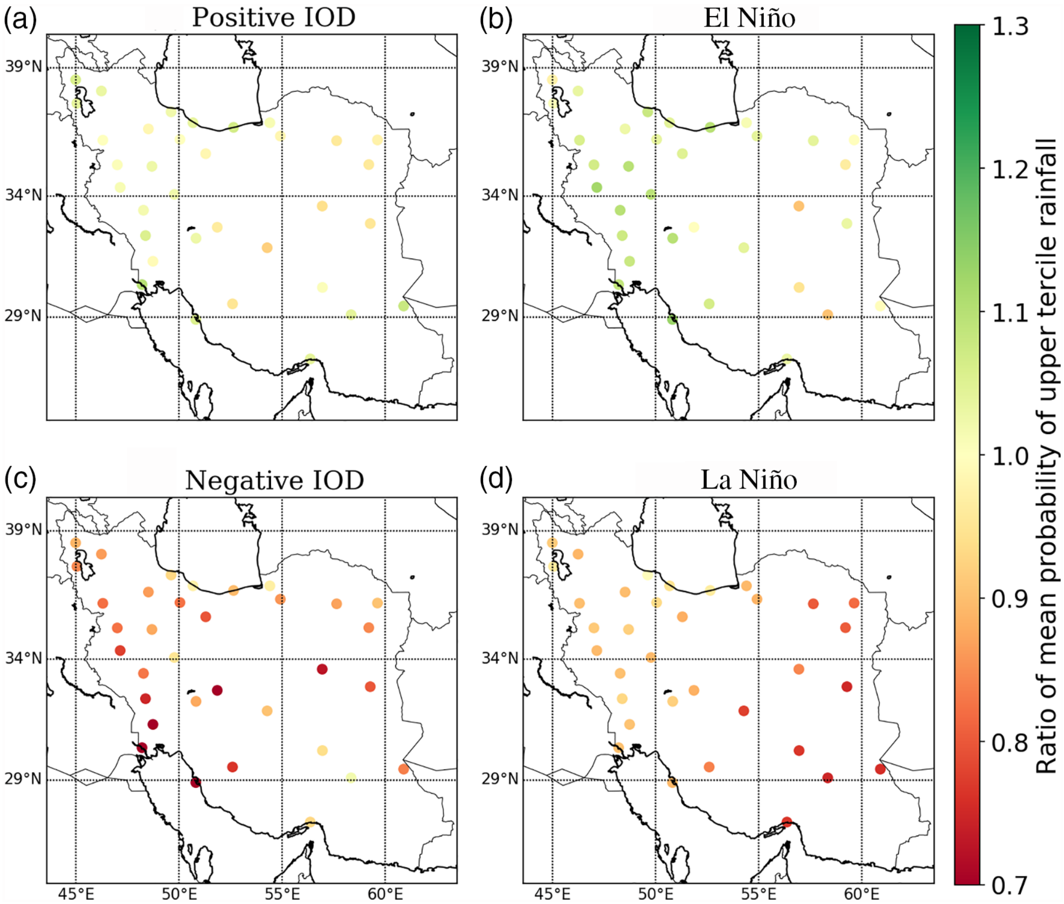

FIGURE 2 Probability of exceeding the upper tercile of daily rainfall for (a) positive IOD; (b) negative IOD; (c) El Niño; (d) La Niña periods, expressed as a ratio to climatological mean probability. Note that this analysis is restricted to the wet season only [Colour figure can be viewed at wileyonlinelibrary.com]

We calculated the probability of the daily rainfall rate exceeding the upper tercile conditioned on the phases of the MJO (amplitude >1), both (a) irrespective of IOD and ENSO states, and (b) considering positive and negative phases of the IOD and ENSO. The conditional probability is presented as a ratio between the probability itself and the probability of the upper tercile rainfall to the baseline probability (e.g., Wheeler *et al.*, 2009) so that values of unity indicate no change in probability of the upper tercile rainfall while values less (greater) than one indicates a reduction (increase) in this probability.

The statistical significances of the results were tested using a Monte Carlo approach whereby we simulated 1,000 randomisations of the MJO phase vector (Wheeler *et al.*, 2009). Each iteration consists of randomly shifting the MJO phase vector relative to the precipitation time series and re-calculating the results as above. Then a confidence interval was built from the many iterations, and if the original result was outside that interval it was deemed statistically significant (at a given significance level). This technique preserves the statistical properties of the MJO such as its serial (auto-) correlation and frequency distribution of days across phases. This tested whether the rainfall probability, by MJO phase, was greater or less than that expected from random climatic variations. We also performed a second significance test of whether changes in the MJO–rainfall relationship during IOD and ENSO states were due to: (a) changes in the rainfall response to the MJO during IOD or ENSO, or (b) changes in the MJO itself, due to its statistical relationship with IOD or ENSO (Ghelani *et al.*, 2017). In this test, we restricted the Monte Carlo phase vector simulation to values from ENSO and the IOD state of interest. With the second test, the changing distribution of MJO phases according to IOD and ENSO states were implicitly taken into account. By performing the second Monte Carlo significance test using only MJO phase values from the IOD and ENSO states of interest, we preserved the MJO–IOD and MJO–ENSO statistical relationships as part of the test. Therefore, the significant results show exceeding the influence of this relationship. Both tests were carried out relative to the 5% statistical significance level. If the results from both tests were statistically significant, we concluded that they could not have arisen due to the MJO–IOD or MJO–ENSO statistical relationship alone and reflect a real change in the MJO–rainfall relationship.

4 | RESULTS

Iran has several different climatic regions across the country. Here we show the probabilities of rainfall for six stations in different climatic regions based on the Köppen–Geiger climate classification (Peel *et al*., 2007). They are Tabriz in the northwest of the country, which has a Mediterranean continental climate; Esfahan in the central region which has a cold desert climate; Rasht in the north which has a warm Mediterranean climate; Shiraz in the south which has a warm semi-arid climate; Ahvaz in the southwest which has a warm desert climate; and Mashhad in the northeast which has a cold semi-arid climate (Figure 1). Figure 3 (left column) shows the probability of non-zero rainfall MJO phases for all years (black lines) and restricted to positive IOD (light-gray bars) and negative IOD (gray bars) periods. The probabilities of rainfall at these stations are higher in phases 1 and 2 and lower in phases 4 and 5. The magnitude of the probability of rainfall variations due to the MJO is greater and more significant at the southern stations (Esfahan, Shiraz, Ahvaz) and less significant for Rasht (northern station) when the IOD is negative. There are large variations in the rainfall probabilities between positive and negative IOD phases during MJO dry (5) and wet (1 and 8) phases. There is less differentiation in rainfall probabilities between El Niño and La Niña phases during dry and wet MJO phases (Figure 3, right column). Specifically, we find that during the negative IOD phase, the MJO has a stronger modulating effect on rainfall during both its wet and dry phases. In relation to ENSO, the magnitude of variations is most pronounced at the southern stations (Esfahan, Shiraz, Ahvaz) and Tabriz during La Niña events and less clear in North stations (Figure 3). There is a larger separation in rainfall probability between ENSO phases during dry (4, 5) and wet (2) MJO phases.

Figure 4 shows the spatial distribution of the probability of wet-season daily rainfall above the upper tercile for MJO phases 1–8, relative to the climatological probability, across all 34 stations. Phases 1 and 2 are wetter than climatology while phases 4 and 5 are drier. The ratio of the probability of the daily rainfall above upper tercile for wet phases (1 and 2) at most stations (except for the northwest region) are >1.25 up to 1.7 (125–170% as likely than climatology) for southwestern stations in phase 1 and decrease for dry phases (4 and 5) with <0.75 at southwest and south stations in phase 4, and down to 0.5 (75–50% as likely than climatology) at south and southeast stations in phase 5. Southwest and southern stations are wetter in phases 7 and 8, with a rainfall probability ratio of 1.25. This is consistent with previous research findings that wet (dry) conditions tend to prevail during MJO phases 1–2 and 7–8 (3–6) over the southern part of Iran. Topography and the direction of moisture flux are important to the rainfall distribution during MJO phases over Iran. When the moisture flux is northwards (onshore), the mountainous areas have larger loading in the west to southeast (Zagros Mountains) than the arid region in central and eastern parts of Iran (Pourasghar *et al*., 2015).

We find that during negative IOD, upper tercile rainfall probabilities significantly increased in MJO phases 1, 2, 3, 7 and 8 and decreased in phases 4–6, and were most

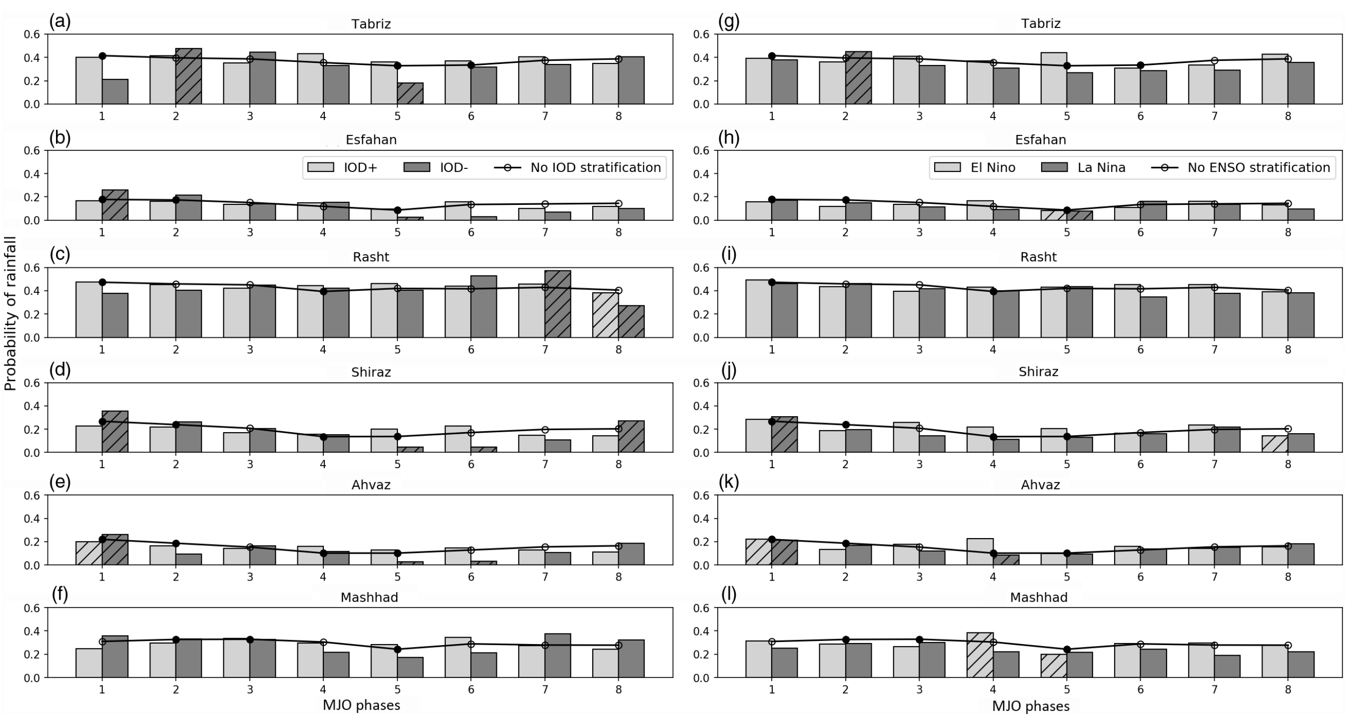

FIGURE 3 Probability of non-zero daily rainfall during the wet season at Tabriz, Esfahan, Rasht, Shiraz, Ahvaz, Mashhad for IOD (left) and ENSO (right) state. All year (black lines), positive IOD (lightgray bars, left), negative IOD (gray bars, left), El Niño (lightgray bars, right), La Niña (gray bars, right). Filled circles and hatched bars indicate the probability in that phase is significantly different (at the 5% level) from the expected probability in random climate, calculated by Monte Carlo randomization of the MJO phase vector

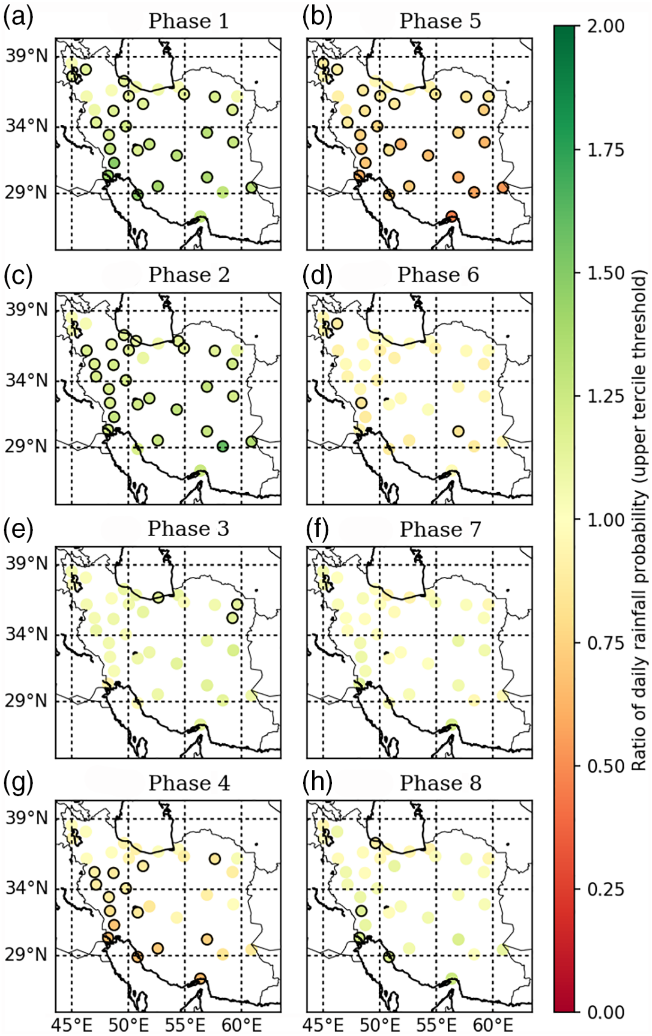

FIGURE 4 Probability of daily wet-season rainfall above the upper tercile for MJO phase 1–8, expressed as a ratio to the climatological probability. Bold circles indicate significant values at the 5% level. (a) Phase 1 (989 days); (b) phase 2 (1,014 days); (c) phase 3 (1,107 days); (d) phase 4 (976 days); (e) phase 5 (1,062 days); (f) phase 6 (1,127 days); (g) phase 7 (985 days); (h) phase 8 (1,121 days) [Colour figure can be viewed at wileyonlinelibrary.com]

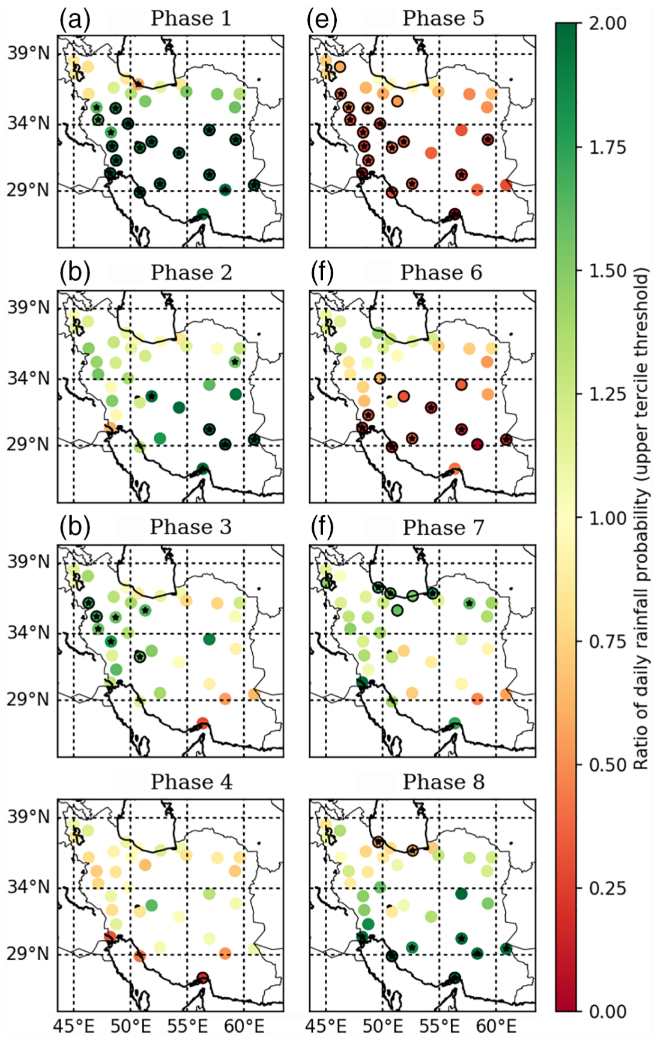

FIGURE 5 Probability of daily wet-season rainfall above the upper tercile for MJO phase 1–8 during negative IOD state, expressed as a ratio to the climatological probability. A bold circled station indicates results significant at the 5% level over the analysis period regardless of IOD state and those flagged with star are additionally significant at 5% level over the analysis period when restricted to negative IOD periods only. (a) Phase 1 (42 days); (b) phase 2 (42 days); (c) phase 3 (49 days); (d) phase 4 (78 days); (e) phase 5 (109 days); (f) phase 6 (66 days); (g) phase 7 (56 days); (h) phase 8 (59 days) [Colour figure can be viewed at wileyonlinelibrary.com]

significant in phases 1, 2 and 5 (stations flagged with stars; Figure 5). During negative IOD, the increased upper tercile rainfall probability ratios were >1.5 up to 2 in MJO phase 1 in the west and southern parts of Iran. The northwest was drier in phase 1 and became wetter in phases 2–3, while the eastern region seemed to get drier in phase 3. The upper tercile rainfall probability ratio decreased from <0.75 down to 0.25 for the southern stations in phase 4. It also decreased in the western region during MJO phase 4 and southern region of Iran during phases 5 and 6. The northwestern region became wetter in phase 6, which seemed to shift to the western and northern regions of Iran in phase 7 and southern region in phase 8. The northern stations were drier in phase 8.

During positive IOD, there was an inconsistent mix of increases and decreases of rainfall probability regionally, with fewer stations showing statistically significant anomalies (Figure 6). Generally, wetter conditions were expected in MJO phase 8. However, during the positive IOD, there was an overall decrease in rainfall probability. Nonetheless, the range of rainfall responses to the MJO and the reduced number of stations showing statistically significant relationships indicate that the MJO–rainfall relationship is suppressed during the positive IOD. In contrast, we found that the MJO-rainfall relationship appears to be enhanced during the negative IOD. The range of rainfall responses to the MJO, expressed as the difference between the largest and smallest probabilities of upper tercile rainfall across all MJO phases, indicates a greater response of rainfall to the MJO during the negative IOD when compared with the positive IOD, and this is particularly significant for the southern

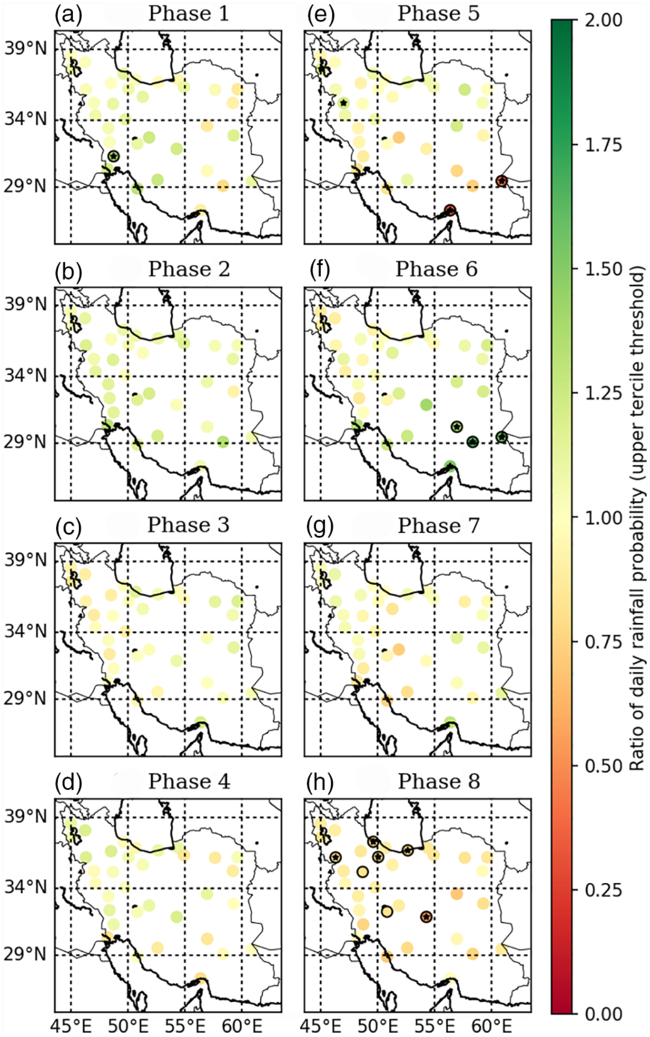

FIGURE 6 Probability of daily wet-season rainfall above the upper tercile for MJO phase 1–8 during positive IOD state, expressed as a ratio to the climatological probability. A bold circled station indicates results significant at the 5% level over the analysis period regardless of IOD state and those flagged with star are additionally significant at 5% level over the analysis period when restricted to positive IOD periods only. (a) Phase 1 (320 days); (b) phase 2 (306 days); (c) phase 3 (297 days); (d) phase 4 (189 days); (e) phase 5 (215 days); (f) phase 6 (224 days); (g) phase 7 (279 days); (h) phase 8 (365 days) [Colour figure can be viewed at wileyonlinelibrary.com]

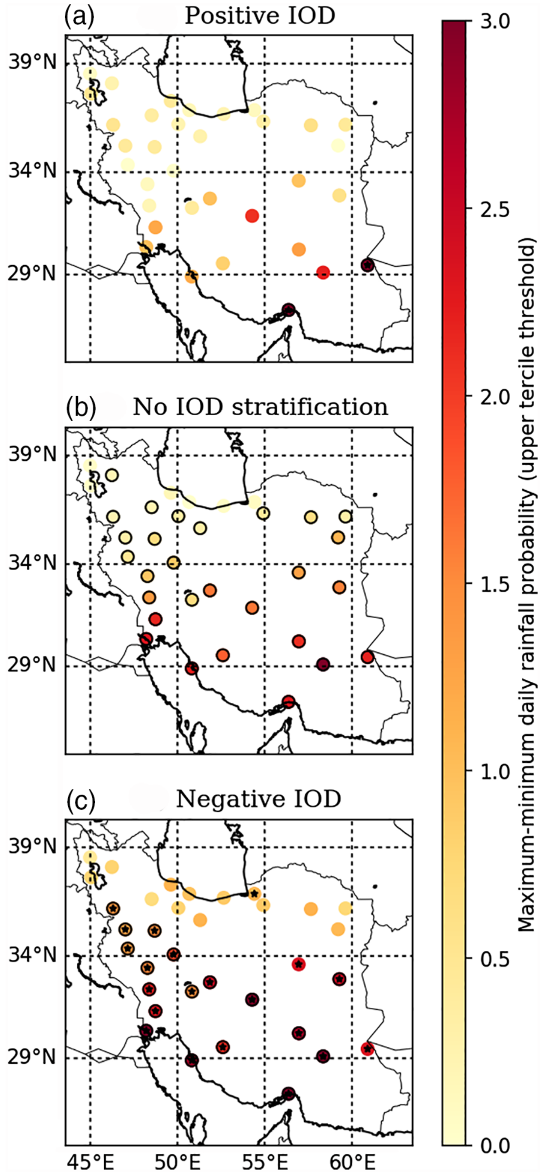

FIGURE 7 Magnitude of the difference between the largest and smallest probability rations of exceeding upper tercile daily rainfall across all MJO phases. The magnitude is shown for (a) positive IOD; (b) all years; (c) negative IOD. A station circled in bold are significant at the 5% level over the analysis period in any of the eight MJO phases and if flagged with star are additionally significant at 5% level over the analysis period when restricted to IOD state [Colour figure can be viewed at wileyonlinelibrary.com]

stations. In contrast, during the positive IOD, the rainfall MJO–rainfall relationship at the southern stations is less than the response observed when not stratified by IOD state (Figure 7).

The sensitivity of the rainfall response to the MJO is greater during La Niña than El Niño (Figures 8 and 9). We found that during La Niña, the upper tercile rainfall probabilities increased in the MJO wetter phases 1 and 2 and decreased in the drier phases 4 and 5 (Figure 8). The increased upper tercile rainfall probability ratios for most stations were about 1.25 corresponding to MJO phases 1–2, and up to 1.7 in the southwest and southern regions of Iran in MJO phase 1. In phase 2, the southeast was drier, which shifts to the southern and western regions in phase 3. Probabilities decreased to <0.75 and down to 0.5 in southern and southwest stations in phase 4 and southeast stations in phase 5. The upper tercile rainfall probabilities increased to nearly 1.25 in southern stations in phases 7 and 8 and >1.5 in southeast stations in phase 7. Significant increases (decreases) in the MJO-rainfall probability relationship were found during wet phases 1 and 2 (dry phase 4 and 5), but only consistently during La Niña years when relating to ENSO. According to the second test, fewer stations were significant compared to the negative IOD state. Conversely, there was an inconsistent mix of increases and decreases in the MJO–rainfall probabilities during El Niño (Figure 9).

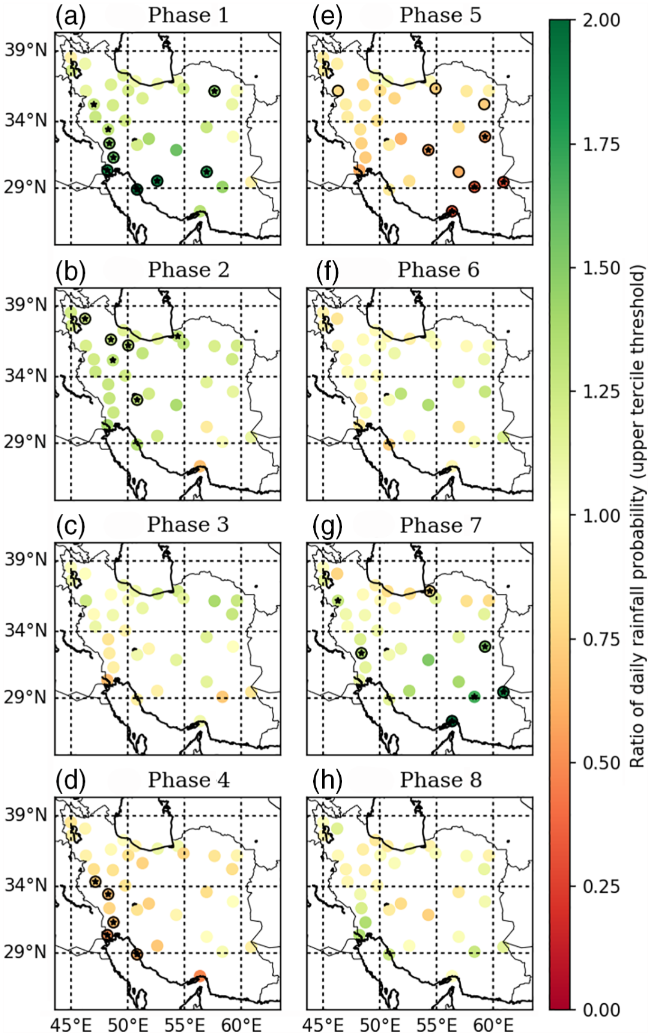

FIGURE 8 Probability of daily wet-season rainfall above the upper tercile for MJO phase 1–8 during La Niña state, expressed as a ratio to the climatological probability. A bold circled station indicates results significant at the 5% level over the analysis period regardless of ENSO state and those flagged with star are additionally significant at 5% level over the analysis period when restricted to La Niña periods only. (a) Phase 1 (140 days); (b) phase 2 (178 days); (c) phase 3 (206 days); (d) phase 4 (247 days); (e) phase 5 (320 days); (f) phase 6 (283 days); (g) phase 7 (184 days); (h) phase 8 (203 days) [Colour figure can be viewed at wileyonlinelibrary.com]

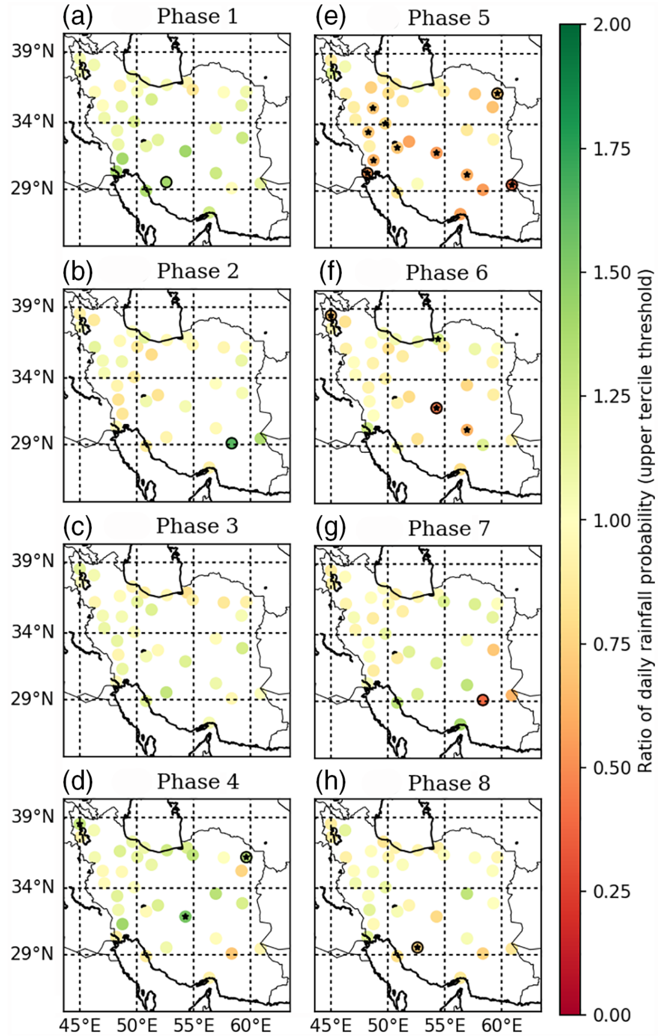

FIGURE 9 Probability of daily wet-season rainfall above the upper tercile for MJO phase 1–8 during El Niño state, expressed as a ratio to the climatological probability. A bold circled station indicates results significant at the 5% level over the analysis period regardless of ENSO state and those flagged with star are additionally significant at 5% level over the analysis period when restricted to El Niño periods only. (a) Phase 1 (214 days); (b) phase 2 (222 days); (c) phase 3 (192 days); (d) phase 4 (151 days); (e) phase 5 (111 days); (f) phase 6 (143 days); (g) phase 7 (155 days); (h) phase 8 (220 days) [Colour figure can be viewed at wileyonlinelibrary.com]

Upper tercile rainfall probabilities significantly decreased to <0.75 and down to 0.5 in southern and southeast stations in MJO phase 5. The relationship between the magnitude of the largest and smallest probabilities of upper tercile rainfall across all MJO phases and phases of ENSO were mostly not significant, except for in the southwest and southern stations during La Niña (Figure 10).

We also examined the variation in the atmospheric variables (RH and vertical velocity) associated with the MJO, corresponding to the separate phases of the IOD and ENSO, to determine if any physical relationships existed with the rainfall response. Composites by MJO phase of RH at 600 hPa, vertical motion (VM) at 300 hPa and PR over Iran are shown in Figures 11 and 12. The RH is higher in phases 1–3 and 7–8, and lower in phases 4–6, in all years (black lines). Moreover, upwards (downwards) VM is evident in phases 1–2 and 7–8 (3–6) which acts to enhance (suppress) the PR in phases 1–2, 7–8 (3–6). These results are also consistent with previous findings which show that MJO phases 1, 2, 7 and 8 favour positive moisture flux anomalies (i.e., an increase) from the Arabian Sea, the Gulf of Aden and Red Sea being transported northwards and onshore into southern Iran, while phases 3–6 favour offshore (i.e., negative) moisture flux anomalies (Pourasghar *et al.*, 2015). The offshore moisture flux reduces the moisture supply from southern Iran. VM anomalies also vary with the eastwards propagation of the MJO. We found that during the negative IOD, the MJO modulation of RH and VM was

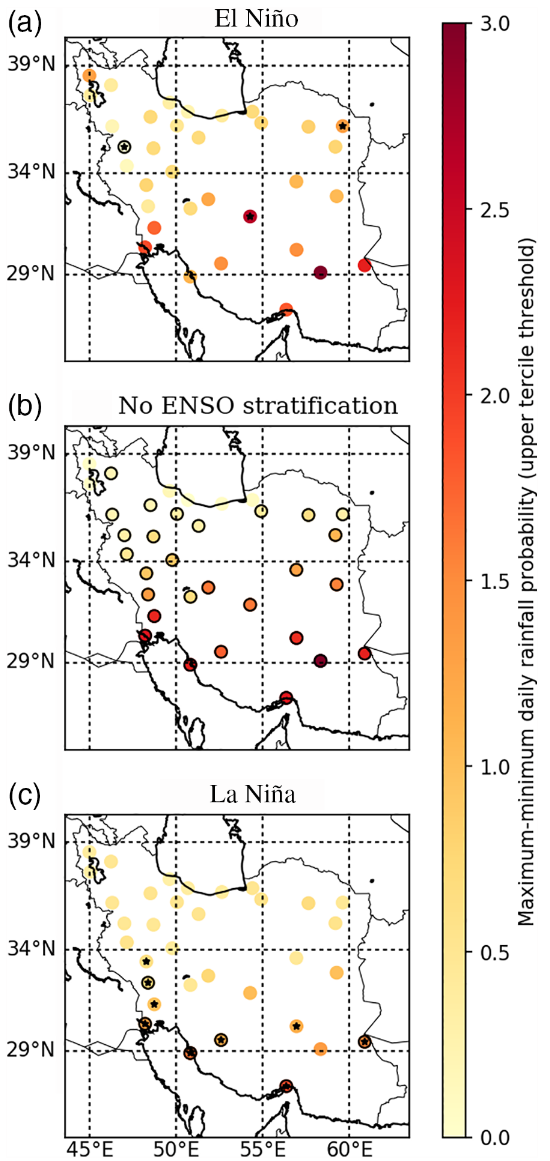

FIGURE 10 Magnitude of the difference between the largest and smallest probability of ratios of exceeding upper tercile daily rainfall across all MJO phases. The magnitude is shown for (a) El Niño; (b) all years; (c) La Niña. A station circled in bold are significant at the 5% level over the analysis period in any of the eight MJO phases and if flagged with star are additionally significant at 5% level over the analysis period when restricted to ENSO state [Colour figure can be viewed at wileyonlinelibrary.com]

stronger than for all years, and stronger than during the positive IOD. The increased (decreased) RH and upwards (downwards) VM enhanced (suppressed) PR in phase 1 (5–6). During the positive IOD, decreased (increased) RH in phases 2–3, 8 and downwards (upwards) VM suppressed (enhanced) PR in theses phases compared to all years. Although the modulation of RH by the MJO over Iran was seen to be stronger during El Niño than La Niña, there was no clear relationship observed with VM (the atmospheric dynamic variable) during El Niño. In contrast during La Niña, despite the reduced RH in phases 1 and 2, upwards motion was seen to enhance PR in these phases, and downwards motion suppressed PR in phases 3–6. During El Niño, reduced RH and downwards VM in MJO phases 2–6 suppressed PR over Iran.

5 | DISCUSSION AND CONCLUSIONS

This study has investigated the influence of the combined effects of the MJO, IOD and El Niño–Southern Oscillation (ENSO) in modulating precipitation variability over Iran. Observed daily precipitation at meteorological stations and atmospheric fields (RH, vertical velocity and PR) from reanalysis data were analysed over Iran during the wet season (October–May) for the 35-year period from 1961 to 2015. The spatial distribution of the probability of daily rainfall above the upper tercile threshold for MJO phases shows that Iran's climate tends to be wetter during MJO phases 1 and 2 and drier during MJO phases 4 and 5. Importantly, we found that the relationship between Iran's wet-season rainfall and the MJO is affected more by the IOD than by ENSO—specifically, negative (positive) IOD states enhance (suppress) the MJO–rainfall relationship. During the negative IOD phase, the MJO increased the probability of upper tercile rainfall more than 2 times in wet phases. On the other hand, the MJO decreased the probability of upper tercile rainfall less than 0.25 times in dry phases. It means that the MJO modulation of daily probability of heavy rainfall (during both wet and dry phases) is larger during the negative IOD phase. During the positive IOD phase, the modulation of heavy rainfall by the MJO is weaker (for both wet and dry phases). The modulation of RH and vertical velocity by the MJO was also found to be stronger during negative IOD phases compared with positive IOD phases. This suggests that the increased (decreased) humidity and upwards (downwards) motion increases (decreases) PRs during the wet (dry) phases. The magnitude of the rainfall response to the MJO during the negative IOD is statistically significant, while the relationship during the positive IOD is weak; and no spatially consistent significant relationship was found during either phase of ENSO.

Large-scale climate modelling studies have shown that the dynamical response of the interaction of the MJO with the IOD and ENSO explains that MJO activity over the Indian Ocean and Maritime Continent tends to be enhanced (suppressed) during the negative (positive) IOD phase (Shinoda and Han, 2005; Wilson *et al.*, 2013; Yuan *et al.*, 2014). No relevant regional dynamical modelling has been performed over Iran. Importantly, this is the first known study to comprehensively investigate the influence of the combined effects of the MJO, IOD and ENSO in modulating precipitation variability in the region using observational data. Numerous previous studies suggest that ENSO impacts inter-annual rainfall variations over Iran (e.g., Nazemosadat and Cordery, 2000; Nazemosadat and Ghasemi, 2004; Raziei *et al.*, 2009; Roghani *et al.*, 2016). We are aware of only one previous

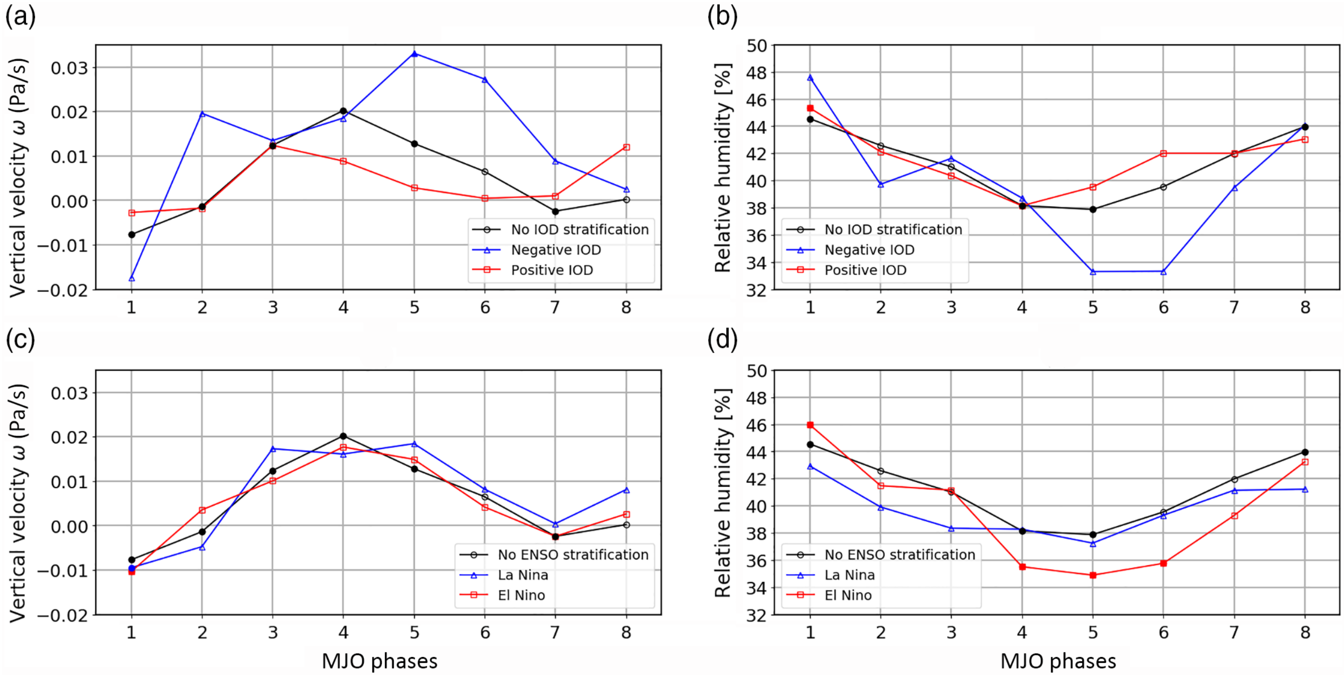

FIGURE 11 (a, c) Composite of RH at 600 hPa and (b, d) composite of vertical velocity at 300 hPa over Iran for MJO phases during all years, negative IOD, positive IOD, La Niña, El Niño. Filled shapes indicate the results in that phase is significantly different (at the 5% level) from the expected in random climate, calculated by Monte Carlo randomization of the MJO phase vector [Colour figure can be viewed at wileyonlinelibrary.com]

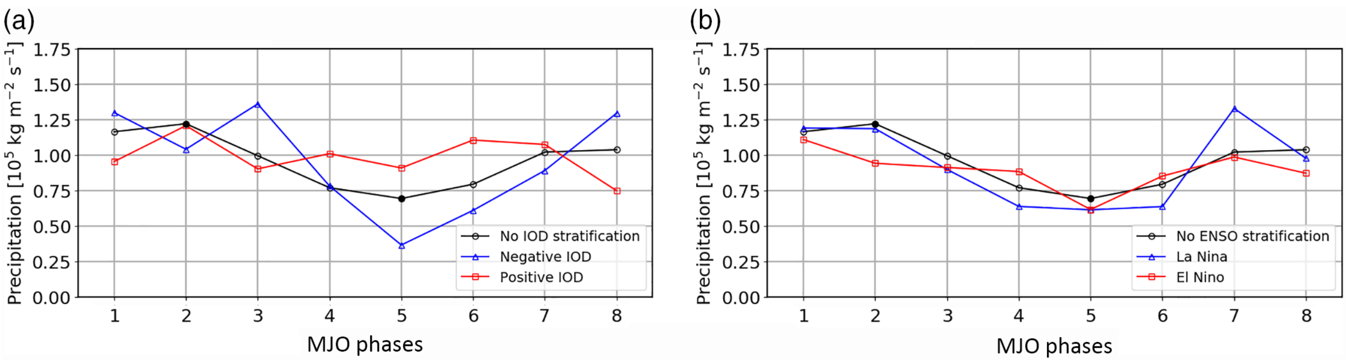

FIGURE 12 Composite of PR over Iran for MJO phases in (a) IOD and (b) ENSO states during all years, negative IOD, positive IOD, La Niña, El Niño. Filled shapes indicate the results in that phase is significantly different (at the 5% level) from the expected in random climate, calculated by Monte Carlo randomization of the MJO phase vector [Colour figure can be viewed at wileyonlinelibrary.com]

study that reports greater importance of IOD compared with ENSO for the region (Pourasghar *et al*., 2012). Our present study highlights that the MJO modulation of rainfall over Iran is jointly dependent on both the IOD and ENSO, but that the IOD is the most important modulating climate mode. This has implications for our understanding of how the MJO modulates rainfall, since the IOD appears to play the dominant role in acting to enhance or suppress it.

Our findings are relevant to future research aiming to improve intra-seasonal forecasts of wet-season rainfall over Iran, whereby improved predictability of the IOD and/or MJO may have beneficial implications for climate and agricultural risk management. However, future numerical modelling studies are required to better understand the physical mechanisms underpinning these connections and to provide more deterministic predictability.

ACKNOWLEDGEMENTS

Daily rainfall data analysed in this article are from the Iran Meteorological Organization. Daily atmospheric reanalysis data analysed here have been provided by the National Centers for Environmental Prediction (NCEP)/National Center for Atmospheric Research (NCAR) Reanalysis. Monthly Niño3 SST index have been provided by National Oceanic and Atmosphere Administration (NOAA) and DMI by Japan

Agency for Marine-Earth Science and Technology (JAMSTEC). The historical reconstruction of the MJO index is available on ECJO's personal website: https://ecjoliver.weebly.com/mjo-reconstruction.html. F.P. acknowledges travel grant funding from the Australian Research Council Centre of Excellence for Climate System Science (ARCCSS). E.C.J.O. was supported by ARCCSS (Grant CE110001028). N.J.H. received funding from the ARC Centre of Excellence for Climate Extremes (Grant CE170100023).

ORCID

Farnaz Pourasghar https://orcid.org/0000-0003-0281-5070

REFERENCES

Alaka, G.J. and Maloney, E.D. (2012) The influence of the MJO on upstream precursors to Africa easterly waves. *Journal of Climate*, 25, 3219–3236. https://doi.org/10.1175/JCLI-D-11-00232.1.

Barlow, M., Zaitchik, B., Paz, S., Black, E., Evans, J. and Hoell, A. (2016) A review of drought in the Middle East and Southwest Asia. *Journal of Climate*, 29, 8547–8574. https://doi.org/10.1175/JCLI-D-13-00692.1.

Compo, G.P., Whitaker, J.S., Sardeshmukh, P.D., Matsui, N., Allan, R.J., Yin, X., Gleason, B.E., Vose, R.S., Rutledge, G., Bessemoulin, P., Brönnimann, S., Brunet, M., Crouthamel, R.I., Grant, A.N., Groisman, P.Y., Jones, P.D., Kruk, M.C., Kruger, A.C., Marshall, G.J., Maugeri, M., Mok, H.Y., Nordli, Ø., Ross, T.F., Trigo, R.M., Wang, X.L., Woodruff, S.D. and Worley, S.J. (2011) The Twentieth Century Reanalysis project. *Quarterly Journal of the Royal Meteorological Society*, 137, 1–28. https://doi.org/10.1002/qj.776.

Ghelani, R.P.S., Oliver, E.C.J., Holbrook, N.J., Wheeler, M.C. and Klotzbach, P. J. (2017) Joint modulation of intraseasonal rainfall in tropical Australia by the Madden–Julian Oscillation and El Niño–Southern Oscillation. *Geophysical Research Letters*, 44, 10754–10761. https://doi.org/10.1002/2017GL075452.

Hendon, H., Wheeler, M. and Zhang, C. (2007) Seasonal dependence of the MJO–ENSO relationship. *Journal of Climate*, 20, 531–543. https://doi.org/10.1175/JCLI4003.1.

Julia, C., Rahn, D.A. and Rutllant, J.A. (2012) Assessing the influence of the MJO on strong precipitation events in subtropical, semi-arid north central Chile. *Journal of Climate*, 25, 7003–7013. https://doi.org/10.1175/JCLI-D-11-00679.1.

Kalnay, E., Kanamitsu, M., Kistler, R., Collins, W., Deaven, D., Gandin, L., Iredell, M., Saha, S., White, G., Woollen, J., Zhu, Y., Chelliah, M., Ebisuzaki, W., Higgins, W., Janowiak, J., Mo, K.C., Ropelowski, C., Wang, J., Leetmaa, A., Reynolds, R., Jenne, R. and Joseph, D. (1996) The NCEP/NCAR 40-year reanalysis project. *Bulletin of the American Meteorological Society*, 77, 437–471. https://doi.org/10.1175/1520-0477(1996)077<0437:TNYRP>2.0.co;2.

Kapur, A. and Zhang, C. (2012) Multiplicative MJO forcing of ENSO. *Journal of Climate*, 25, 8132–8147. https://doi.org/10.1175/JCLI-D-11-00609.1.

Khalili, K., Tahoudi, M.N., Mirabbasi, R. and Ahmadi, F. (2016) Investigation of spatial and temporal variability of precipitation in Iran over last half century. *Stochastic Environmental Research Risk Assessment*, 30, 1205–1221. https://doi.org/10.1007/s00477-015-1095-4.

Lin, A. and Li, T. (2008) Energy spectrum characteristics of boreal and summer intraseasonal oscillation: climatology and variations during ENSO developing and decaying phases. *Journal of Climate*, 21, 6304–6320. https://doi.org/10.1175/2008JCLI2331.1.

Madani, K. (2014) Water management in Iran: what is causing the looming crisis? *Journal of Environmental Studies and Sciences*, 4, 315–328. https://doi.org/10.1007/s13412-014-0182-z.

Nazemosadat, M.J. and Cordery, I. (2000) On the relationships between ENSO and autumn rainfall in Iran. *International Journal of Climatology*, 20, 47–61. https://doi.org/10.1002/(SICI)1097-0088(200001)20:1<47::AID-JOC461>3.0.CO;2-P.

Nazemosadat, M.J. and Ghasemi, A.R. (2004) Quantifying the ENSO-related shifts in the intensity and probability of drought and wet periods in Iran. *Journal of Climate*, 17, 4005–4018. https://doi.org/10.1175/1520-0442(2004)017<4005:QTESIT>2.0.CO;2.

Nazemosadat, M.J., Samani, N., Barry, D.A. and Molaii, N.M. (2006) ENSO forcing on climate change in Iran: precipitation analysis. *Iranian Journal of Science and Technology*, 30, 555–565. https://doi.org/10.22099/IJSTC.2006.780.

Nazemosadat, M.J. and Shahgholian, K. (2017) Heavy precipitation in the southwest of Iran: association with the Madden–Julian Oscillation and synoptic scale analysis. *Climate Dynamics*, 49, 3091–3109. https://doi.org/10.1007/s00382-016-3496-6.

Oliver, E.C.J. (2016) Blind use of reanalysis data: apparent trends in Madden–Julian Oscillation activity driven by observational changes. *International Journal of Climatology*, 36, 3458–3468. https://doi.org/10.1002/joc.4568.

Oliver, E.C.J. and Thompson, K.R. (2012) A reconstruction of Madden–Julian Oscillation variability from 1905 to 2008. *Journal of Climate*, 25, 1996–2019. https://doi.org/10.1175/JCLI-D-11-00154.1.

Pai, D.S., Jyoti, B., Sreejith, O.P. and Hatwar, H.R. (2011) Impact of MJO on the intraseasonal variation of summer monsoon rainfall over India. *Climate Dynamics*, 36, 41–55. https://doi.org/10.1007/s00382-009-0634-4.

Peel, M.C., Finlayson, B.L. and Mcmahon, T.A. (2007) Updated world map of the Köppen–Geiger climate classification. *Hydrology and Earth System Science*, 11, 1633–1644. https://doi.org/10.5194/hess-11-1633-2007.

Pohl, B. and Matthews, A.J. (2007) Observed changes in the life time and amplitude of the Madden–Julian Oscillation associated with interannual ENSO sea surface temperature anomalies. *Journal of Climate*, 20, 2659–2674. https://doi.org/10.1175/JCLI4230.1.

Pourasghar, F., Tozuka, T., Ghaemi, H., Oettli, P., Jahanbakhsh, S. and Yamagata, T. (2015) Influences of the MJO on intraseasonal rainfall variability over southern Iran. *Atmospheric Science Letters*, 16, 110–118. https://doi.org/10.1002/asl2.531.

Pourasghar, F., Tozuka, T., Jahanbakhsh, S., Sari Sarraf, B., Ghaemi, H. and Yamagata, T. (2012) The interannual precipitation variability in the southern part of Iran as linked to large-scale climate modes. *Climate Dynamics*, 39, 2329–2341. https://doi.org/10.1007/s00382-012-1357-5.

Raziei, T., Mofidi, A., Santos, J.A. and Bordi, I. (2012) Spatial patterns and regimes of daily precipitation in Iran in relation to large-scale atmospheric circulation. *International Journal of Climatology*, 32, 1226–1237. https://doi.org/10.1002/joc.2347.

Raziei, T., Saghafian, B., Paulo, A.A., Pereira, L. and Bordi, I. (2009) Spatial patterns and temporal variability of drought in western Iran. *Water Resources Management*, 23, 439–455. https://doi.org/10.1007/s11269-008-9282-4.

Roghani, R., Soltani, S. and Bashari, H. (2016) Influence of Southern Oscillation on autumn rainfall in Iran (1951–2011). *Theoretical Applied Climatology*, 124, 411–423. https://doi.org/10.1007/s00704-015-1423.0.

Rousta, I., Soltani, M., Zhou, W. and Cheung, H.H.N. (2016) Analysis of extreme precipitation events over central plateau of Iran. *American Journal of Climate Change*, 5, 297–313. https://doi.org/10.4236/ajcc.2016.53024.

Saji, N.H., Goswami, B.N., Vinayachandran, P.N. and Yamagata, T. (1999) A dipole mode in tropical Indian Ocean. *Nature*, 401, 360–363. https://doi.org/10.1038/43854.

Seiki, A. and Takayabu, Y.N. (2007) Westerly wind bursts and their relation with intraseasonal variations and ENSO part I: statistics. *Monthly Weather Review*, 135, 3325–3345. https://doi.org/10.1175/MWR3477.1.

Shinoda, T. and Han, W. (2005) Influence of Indian Ocean Dipole on atmospheric subseasonal variability. *Journal of Climate*, 18, 3891–3909. https://doi.org/10.1175/JCLI3510.1.

Soltani, S., Saboohi, S. and Yaghmaei, L. (2012) Rainfall and rainy days trend in Iran. *Climate Change*, 110, 187–213. https://doi.org/10.1007/s10584-011-0146-1.

Wheeler, M.C. and Hendon, H. (2004) An all-season real-time multivariate MJO index: development of an index for monitoring and prediction. *Monthly Weather Review*, 132, 1917–1932. https://doi.org/10.1175/1520-0493/92004)132<1917:AARMMI>2.0.CO;2.

Wheeler, M.C., Hendon, H.H., Cleland, S., Meinke, H. and Donald, A. (2009) Impact of the Madden–Julian Oscillation on Australian rainfall and circulation. *Journal of Climate*, 22, 1482–1498. https://doi.org/10.1175/2008JCLI2595.1.

Wilson, E.A., Gordon, A.L. and Kim, D. (2013) Observations of the Madden–Julian Oscillation during Indian Ocean Dipole events. *Journal of Geophysical Research*, 118, 2588–2599. https://doi.org/10.1002/jgrd.50241.

Yuan, Y., Yang, H. and Li, C.Y. (2014) Possible influences of the tropical Indian Ocean Dipole on the eastward propagation of MJO. *Journal of Tropical Meteorology*, 20, 173–180 1006-8775(2014) 02-0173-08.

Zhang, C. (2005) Madden–Julian Oscillation. *Reviews of Geophysics*, 43, 1–36. https://doi.org/10.1029/2004RG000158.

How to cite this article: Pourasghar F, Oliver ECJ, Holbrook NJ. Modulation of wet-season rainfall over Iran by the Madden–Julian Oscillation, Indian Ocean Dipole and El Niño–Southern Oscillation. *Int J Climatol*. 2019;1–12. https://doi.org/10.1002/joc.6057